

Analysis of Bit Error Probability for Imperfect Timing Synchronization in Virtual MISO Networks

Muddassar Hussain and Syed Ali Hassan

School of Electrical Engineering & Computer Science (SECS)

National University of Sciences & Technology (NUST), Islamabad, Pakistan 44000

Email: {muddassar.hussain, ali.hassan}@seecs.edu.pk

Abstract—This paper considers a virtual multiple-input single-output (VMISO) network, where spatially separated single-antenna radios cooperatively transmit the same data to a destination. The existing works for the VMISO system assume perfect synchronization between the nodes. However, in this paper, we investigate the effects of imperfect timing synchronization on the performance of this network. For that purpose, we develop a statistical model for the timing errors and derive the expressions for the bit error probability (BEP) using this model. The results indicate that the BEP performance is degraded due to imperfect timing synchronization and the BEP is dependent upon the number of radios per cluster, signal-to-noise ratio (SNR) and the distance disparities between the nodes.

I. INTRODUCTION

Cooperative transmission (CT) has emerged as one of the most promising techniques to combat the multi-path fading [1]. In a CT-based network, same data is transmitted by spatially separated radios via uncorrelated fading channels, thereby providing the transmit diversity. This form of cooperation is not only suitable for cellular networks but also for sensor and ad hoc networks. CT has shown considerable advantages in terms of energy-efficiency [2], opportunistic routing [3] and range extension [4], which make it very suitable to be used in wireless sensor networks (WSNs). In WSNs, the sensor nodes are distributed in an area and a group of nodes transmit the same message to a destination or another group of nodes. Thus the data is propagated as virtual multiple-input single-output (VMISO) until the destination is reached [5]. Although, this scheme provides diversity and array gains, however, full diversity can only be achieved if all the replicas of the data transmitted by a group of nodes are perfectly aligned at the receiver, i.e., perfect timing synchronization. Most of existing works in this area rely on the perfect timing synchronization such that the coherent diversity combining techniques, e.g., maximal-ratio combining (MRC) can be used [6] [7].

Several schemes have been proposed for the timing synchronization of the cooperative diversity systems. In [8], a timing synchronization scheme is presented for a cooperative network in which a source broadcasts its data to the relays that cooperatively transmit it towards the destination. In [9], a receiver timing as well as carrier frequency synchronization

is proposed for the network resembling to the one assumed in [8]. The perfect synchronization in a cooperative network cannot be achieved due to the distributed nature of these systems, thereby causing the timing and carrier frequency synchronization errors [8]. Although [8] and [9] present estimators for the timing offsets in single-input single-output (SISO) and the VMISO networks, however, the effects of the imperfect synchronization are not catered for evaluating the system performance.

Analytical and simulation results on the performance of the SISO system in the presence of timing synchronization errors have been presented in [10]. The analytical expression for bit error rate (BER) is derived for the binary phase shift keying (BPSK) modulation with rectangular pulse-shaping and quasi-static flat Rayleigh fading channel. Moreover, it is assumed that the variance of the timing synchronization errors is not dependent on signal-to-noise ratio (SNR). The result shows that a slight increase in the variance of the timing synchronization error causes a huge increase in the BER of the system. Moreover, the BER performance of the SISO system with generalized M-ary phase shift keying (MPSK) under imperfect phase or timing synchronization is given in [11]. The authors assume an additive white Gaussian noise (AWGN) channel, however, the multi-path fading is not considered. Similarly, the performance of a VMISO system under imperfect timing synchronization is analyzed in [12]. The authors consider a VMISO system with transmit beam-forming and Rayleigh fading channel. The results show that an increase in the timing error causes a huge deterioration in the BER performance of the system and the diversity gain can vanish altogether if the timing error becomes greater than 80% of the symbol duration. However, the authors do not provide any expression for the BER of the system in this work.

In a multi-hop cooperative network, the source broadcasts its data to relays, which cooperatively propagate the data towards the destination. The broadcast of the data from the source to the relays can be considered as a SISO system, while the cooperative transmission by the relays can be viewed as a VMISO system. In this paper, we intend to analyze and quantify the effects of timing synchronization errors on the performance of VMISO system and include SISO network as a special case. This analysis can be used to analyze the performance of multi-hop cooperative networks, which is the main motivation behind this study. We develop a novel

This work was supported by the National ICT R&D Fund, Pakistan.

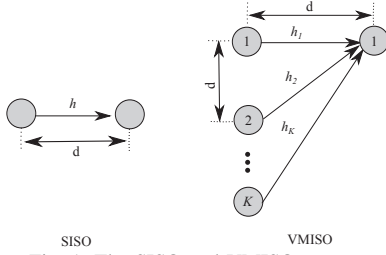


Fig. 1: The SISO and VMISO system.

mathematical model to study the statistics of the timing errors and derive the expressions for the bit error probability (BEP) of the SISO and VMISO systems operating under imperfect timing synchronization.

The rest of this paper is organized as follows. In Section II, the system model is described. Section III derives the statistics of the timing synchronization error. Section IV provides the expressions for the worst-case BEP. Section V provides the analytical and simulation results. The paper is concluded in Section VI.

II. SYSTEM MODEL

We consider the SISO and VMISO systems shown in Fig. 1. The SISO system consists of a single transmitter which is d distance apart from its receiver, while the VMISO system consists of K transmitters and a single receiver. Each transmitting node in VMISO system is d distance apart from its adjacent transmitting node. Without the loss of generality we assume that the receiving node in VMISO is at a distance d apart from the first transmitting node as shown in Fig. 1. The distance of receiver from the rest of the transmitting nodes can be simply found by using the Euclidian geometry. We assume a quasi-static Rayleigh flat fading channel. Furthermore, the channel coefficient between any two nodes is assumed to follow a complex normal distribution with zero mean and σ_h^2 variance. The channel coefficients are assumed to be independent and identically distributed (i.i.d).

Before the transmission of data, each transmitter transmits its training sequence to the relevant receiver. The receiver then estimates the timing offset(s) by using either the maximum likelihood (ML)-based single timing offset estimation algorithm for the SISO system or ML-based multiple timing offset estimation algorithm for the VMISO system given in [8] and [9]. Afterwards, the receiver pre-synchronizes its clock by using the estimated timing offset and channel state information (CSI). After the completion of synchronization and training phase, the actual data is transmitted.

III. STATISTICS OF TIMING ERROR

In this section, our aim is to find the statistics of the timing synchronization errors, which occur in the SISO and VMISO systems. We deal them separately in the following subsections.

A. The timing error in the SISO system

In the case of SISO system, the received signal experiences a propagation delay, τ , which is proportional to the distance

between the transmitter and the receiver. At the receiver, the received signal is compensated for the timing offset by sampling with the receiver clock delayed by $\hat{\tau}T$, where $\hat{\tau}$ is the estimated timing offset. This $\hat{\tau}$ is estimated according to the ML-based estimator for a general SISO system as described in [8]. Assuming that the estimation is unbiased, we have $\hat{\tau} \sim \mathcal{N}(\tau, \sigma_1^2)$, where σ_1^2 is the variance of the estimator for the SISO link. This σ_1^2 is inversely proportional to SNR i.e., $\sigma_1^2 \approx c_1(L_o)N_o/E_s$, where $c_1(L_o)$ is a constant, which is related to the length of the training sequence, L_o . The E_s is the symbol energy and N_o is the variance of the AWGN. The timing error for the SISO link is $\epsilon = \tau - \hat{\tau}$. Because $\hat{\tau} \sim \mathcal{N}(\tau, \sigma_1^2)$, therefore, $\epsilon \sim \mathcal{N}(0, \sigma_1^2)$.

B. The timing error in the VMISO system

Contrary to the SISO system, the received signal in a generic VMISO system consists of a sum of K transmitted signals, each having a distinct timing offset. We denote the timing offset corresponding to the signal transmitted by the k^{th} node by τ_k . At the receiver, all the timing offsets are estimated by using the ML-based estimator as described in [8]. In order to optimally sample the signal, a single sampling time is obtained by combining all the estimated offsets, $\{\hat{\tau}_1, \hat{\tau}_2, \dots, \hat{\tau}_K\}$. The received signal is sampled by delaying the clock of the receiver by $\hat{\tau}T$, where

$$\hat{\tau} = \sum_{k=1}^K \beta_k \hat{\tau}_k, \quad (1)$$

where, $\beta_k = |h_k|^2 / \sum_{j=1}^K |h_j|^2$. The h_k is the complex channel coefficient between the k^{th} transmitter and the receiver. As previously, $\hat{\tau}_k \sim \mathcal{N}(\tau_k, \sigma_2^2)$. σ_2^2 represents the variance of the estimator for the VMISO case and $\sigma_2^2 \approx c_2(L_o, K)N_o/E_s$, where $c_2(L_o, K)$ is a constant related to the length of the training sequence, L_o , and the number of relays per cluster, K [8]. The mean of $\hat{\tau}$ can be found by applying expectation operator on (1) and is given as

$$\mu_{\hat{\tau}} = \sum_{k=1}^K \mathbb{E}[\beta_k] \mathbb{E}[\hat{\tau}_k], \quad (2)$$

where $\mathbb{E}[\cdot]$ represents the expectation operator. By using the conclusion provided in [13] and the properties of the distribution of $|h_k|^2$, we have $\mathbb{E}[\beta_k] = 1/K$. Hence, the mean of $\hat{\tau}$ can be found as

$$\mu_{\hat{\tau}} = \frac{1}{K} \sum_{k=1}^K \tau_k. \quad (3)$$

From the above equation, we can see that the mean of the estimated timing offset is simply the mean of the propagation delays. The timing error corresponding to the signal transmitted by the k^{th} node is $\epsilon_k = \tau_k - \hat{\tau}$. By using (3), the mean of ϵ_k is given as

$$\mu_{\epsilon_k} = \tau_k - \frac{1}{K} \sum_{k=1}^K \tau_k, \quad (4)$$

while the variance of $\hat{\tau}$ is given as

$$\sigma_{\hat{\tau}}^2 = \mathbb{E}[\hat{\tau}^2] - (\mathbb{E}[\hat{\tau}])^2. \quad (5)$$

The first term in (5) can be written as

$$\mathbb{E}[(\hat{\tau})^2] = \mathbb{E}\left[\left(\sum_{k=1}^K \beta_k \hat{\tau}_k\right)^2\right]. \quad (6)$$

It has been shown in Appendix A that (6) can be evaluated as

$$\mathbb{E}[\hat{\tau}^2] = \frac{2}{K(K+1)} \sum_{k=1}^K (\sigma_2^2 + \tau_k^2) + \frac{1}{K(K+1)} \sum_{p=1}^K \sum_{\substack{q=1 \\ q \neq p}}^K \tau_p \tau_q. \quad (7)$$

By substituting from (3) and (7) into (5), we get

$$\begin{aligned} \sigma_{\hat{\tau}}^2 &= \frac{2}{K(K+1)} \sum_{k=1}^K (\sigma_2^2 + \tau_k^2) \\ &+ \frac{1}{K(K+1)} \sum_{p=1}^K \sum_{\substack{q=1 \\ q \neq p}}^K \tau_p \tau_q - \frac{1}{K^2} \left(\sum_{k=1}^K \tau_k\right)^2. \end{aligned} \quad (8)$$

It should be noted that the variance of the timing error ϵ_k is identical to $\sigma_{\hat{\tau}}^2$ i.e., $\sigma_{\epsilon_k}^2 = \sigma_{\hat{\tau}}^2 \forall k = \{1, 2, \dots, K\}$.

IV. BEP ANALYSIS

In this section, we derive the BEP expression for both the SISO and VMISO systems, which can be used along with the statistics of timing errors to analyze the performance of these systems. Although the BEP of SISO system has been analyzed in [9], we first derive a variant of SISO BEP, which incorporates not only the worst-case signaling scenario employing root-raised cosine pulse-shaping but also includes the statistics of timing errors as derived in Section III. We then carry forward this analysis to a more general MISO case.

A. The worst-case BEP for the SISO system

For a general SISO system, the complex envelope of the received signal is given as

$$r(t) = h \sum_{i=-\infty}^{\infty} s(i)g(t - iT - \tau T) + n(t), \quad (9)$$

where τ is the normalized timing delay proportional to the distance between the transmitter and receiver, h is the channel coefficient, which is assumed to follow a complex normal distribution with zero mean and σ_h^2 variance and $n(t)$ is the complex AWGN with variance N_o . The function $g(t)$ denotes a raised cosine pulse with tail truncated at $t = \pm L_g T$ [14], where T is the symbol duration. The i^{th} transmitted symbol, $s(i)$, is a complex valued symbol from the QPSK constellation with $\mathbb{E}[|s(i)|^2] = E_s$. Although, QPSK is a quaternary modulation scheme, it can also be interpreted as two independently modulated BPSK waveforms each modulating odd (or even) bits [15]. Therefore, we can represent the above QPSK signal as sum of two BPSK signals, i.e., $r(t) = r_1 + jr_2$, where r_1 and r_2 are given as

$$r_1(t) = h\sqrt{E_s} \sum_{i=-\infty}^{\infty} \cos(\theta_i)g(t - iT - \tau T) + n_I(t), \quad (10)$$

$$r_2(t) = h\sqrt{E_s} \sum_{i=-\infty}^{\infty} \sin(\theta_i)g(t - iT - \tau T) + n_Q(t), \quad (11)$$

and $n(t) = n_I(t) + jn_Q(t)$. The symbols n_I and n_Q represents the In-phase and Quadrature components of the AWGN, respectively. Because the BPSK signals r_1 and r_2 can be treated independently, the BEP of either of the two signals is equal to the BEP of QPSK. Therefore, in this section, the BEP for r_1 is derived only. The received signal is sampled with receiver clock delayed by $\hat{\tau}T$ to compensate for the timing offset. After sampling, the received signal r_1 can be given as

$$r_1[m] = h\sqrt{E_s} \sum_{i=-L_g+m}^{L_g+m} \cos(\theta_i)g((m-i)T - \epsilon T) + n_I[m]. \quad (12)$$

It should be noted that the index of the summation in (12) is $i = \{-L_g + m, -L_g + m + 1, \dots, L_g + m\}$ because the tail of $g(t)$ is truncated at $t = \pm L_g T$. At the receiver, the amplitude of desired signal is decreased due to the timing error, ϵ . However, the amount of degradation in the amplitude of the desired signal is also dependent upon the phase of bits transmitted in interval $(-L_g + m)T \leq t \leq (L_g + m)T$. The worst-case scenario occurs when the amplitude of the sample corresponding to m^{th} bit is minimized, i.e., when the adjacent bits are antipodal. The received signal for such a case is given as

$$\tilde{r}_1[m] = h\sqrt{E_s}\xi(\epsilon)\cos(\theta_m) + n_I[m], \quad (13)$$

where

$$\xi(\epsilon) = g(-\epsilon T) - \sum_{\substack{i=-L_g+m \\ i \neq m}}^{L_g+m} |g((m-i)T - \epsilon T)|. \quad (14)$$

For the case of perfect synchronization, the conditional bit error probability can be expressed as

$$\mathbb{P}_{lb}(e; h) = \frac{1}{2} \operatorname{erfc}\left(\sqrt{\frac{|h|^2 E_b}{N_o}}\right), \quad (15)$$

where the subscript lb denotes the lower-bound case, $\operatorname{erfc}(\cdot)$ is the complementary error function and $E_b = E_s/2$. Since the correlator output is decreased by $\xi(\epsilon)$ due to timing error, therefore, the worst-case BEP for imperfect synchronization is given as

$$\mathbb{P}(e; h, \epsilon) = \frac{1}{2} \operatorname{erfc}\left(\sqrt{\frac{|h|^2 E_b}{N_o}} \xi(\epsilon)\right). \quad (16)$$

We can find $\mathbb{P}(e; \epsilon)$ by marginalizing $\mathbb{P}(e; h, \epsilon)$ over the probability density function (PDF) of $|h|^2$. If channel coefficient, $h \sim \mathcal{CN}(0, \sigma_h^2)$, then $|h|^2 \sim \text{Exponential}(\sigma_h^2)$. Hence, the PDF of $|h|^2$ can be given as

$$f_{|h|^2}(x) = \frac{1}{\sigma_h^2} \exp\left(-\frac{x}{\sigma_h^2}\right). \quad (17)$$

Therefore,

$$\mathbb{P}(e; \epsilon) = \frac{1}{2} \int_0^{\infty} \operatorname{erfc}(\sqrt{x\gamma_b}\xi(\epsilon)) f_{|h|^2}(x) dx, \quad (18)$$

where $\bar{\gamma}_b = E_b/N_o$. After evaluating the integral in (18), $\mathbb{P}(e; \epsilon)$ can be given as

$$\mathbb{P}(e; \epsilon) = \frac{1}{2} \left(1 - \xi(\epsilon) \sqrt{\frac{\sigma_h^2 \bar{\gamma}_b}{1 + \sigma_h^2 \bar{\gamma}_b (\xi(\epsilon))^2}} \right). \quad (19)$$

The timing error, ϵ , follows a normal distribution with zero mean and σ_1^2 variance, i.e., $\epsilon \sim \mathcal{N}(0, \sigma_1^2)$. The unconditional BEP, $\mathbb{P}(e)$ is found by averaging $\mathbb{P}(e; \epsilon)$ over the PDF of ϵ is given as

$$\mathbb{P}(e) = \frac{1}{2} - \frac{1}{2} \int_{-\infty}^{\infty} \xi(x) \sqrt{\frac{\sigma_h^2 \bar{\gamma}_b}{1 + \sigma_h^2 \bar{\gamma}_b (\xi(x))^2}} f_\epsilon(x) dx. \quad (20)$$

where, $f_\epsilon(x)$ is the PDF of timing error, ϵ . The integration in the above equation is tedious to evaluate analytically, however can be solved numerically by using the numerical integral routines. Using a method similar to imperfect synchronization case, we can derive the unconditional BEP for the perfectly synchronized receiver and is given as

$$\mathbb{P}_{tb}(e) = \frac{1}{2} \left(1 - \sqrt{\frac{\sigma_h^2 \bar{\gamma}_b}{1 + \sigma_h^2 \bar{\gamma}_b}} \right). \quad (21)$$

B. The worst-case BEP for the VMISO system

In this section, the BEP of the VMISO system with the imperfect synchronization is derived. Assuming perfect CSI, the signal at the receiver relay after coherent combining can be given as

$$y(t) = \sum_{k=1}^K |h_k|^2 \sum_{i=-\infty}^{\infty} s(i) g(t - iT - \tau_k T) + n(t). \quad (22)$$

We use the same argument as given in SISO case and derive the BEP for either of the two BPSK signals resulted from the decomposition of above QPSK signal. One of the BPSK signals is given as

$$y_1(t) = \sqrt{E_s} \sum_{k=1}^K |h_k|^2 \sum_{i=-\infty}^{\infty} \cos(\theta_i) g(t - iT - \tau_k T) + n_I(t). \quad (23)$$

Upon reception, the signal is compensated for the timing offset by sampling with the receiver clock delayed by $\hat{\tau}T$. For decoding the m^{th} bit, the received signal is given as

$$y_1[m] = \sqrt{E_s} \sum_{k=1}^K |h_k|^2 \sum_{i=-L_g+m}^{L_g+m} \cos(\theta_i) g((m-i)T - (\tau_k - \hat{\tau})T) + n_I[m],$$

For worst case, we can express the above signal as

$$\tilde{y}_1[m] = \sqrt{E_s} \sum_{k=1}^K |h_k|^2 \xi(\tau_k - \hat{\tau}) \cos(\theta_m) + n_I[m]. \quad (24)$$

The worst-case conditional BEP is given as

$$\mathbb{P}(e; \hat{\tau}, \mathbf{h}) = \frac{1}{2} \text{erfc} \left(\sqrt{\frac{E_b}{N_o}} \sum_{k=1}^K |h_k|^2 \xi(\tau_k - \hat{\tau}) \right), \quad (26)$$

where $\mathbf{h} = [h_1, h_2, \dots, h_K]^T$. Before proceeding further, we consider the following lemma.

Lemma 1. Let X_1, X_2, \dots, X_N be i.i.d exponential random variables having identical mean μ and $X = a_1 X_1 + a_2 X_2 + \dots + a_N X_N$, where $a_i \in \mathbb{R} \forall i = 1, 2, \dots, N$. The PDF of X is given as

$$f_X(x) = \sum_{i=1}^N \frac{a_i^{N-2} \text{sign}(\frac{1}{a_i}) \exp(-\frac{x}{a_i \mu}) u(x \text{sign}(\frac{1}{a_i}))}{\mu \prod_{l=1, l \neq i}^N (a_l - a_i)}, \quad (27)$$

where

$$\text{sign}(z) = \begin{cases} 1 & z > 0 \\ -1 & z < 0 \\ 0 & z = 0. \end{cases} \quad (28)$$

Proof. The Characteristic Function (CF) of X is the product of CF of $X_i \forall i = \{1, 2, \dots, N\}$ and is given as

$$\varphi(t) = \frac{1}{\prod_{i=1}^N (1 - j a_i \mu t)}. \quad (29)$$

By using partial fractions, the CF defined in (29) can be written as

$$\varphi(t) = \sum_{i=1}^N \frac{a_i^{N-1}}{(1 - j a_i \mu t) \prod_{l=1, l \neq i}^N (a_l - a_i)}. \quad (30)$$

By applying Inverse Fourier Transform to the CF given in (30), the PDF of X is found, which is given in (27). ■

Based upon the above lemma and (26), we have following theorem

Theorem 1. For a VMISO system with Rayleigh flat fading channel and imperfect synchronization, the worst-case conditional BEP, $\mathbb{P}(e; \hat{\tau})$ is given as

$$\begin{aligned} \mathbb{P}(e; \hat{\tau}) &= \frac{1}{2} \sum_{i=1}^K \alpha_i \left[1 - \exp\left(\frac{1}{4\sigma_h^4 (\xi(\tau_i - \hat{\tau}))^2 \bar{\gamma}_b}\right) \text{erfc}\left(\frac{1}{2\sigma_h^2 \xi(\tau_i - \hat{\tau}) \sqrt{\bar{\gamma}_b}}\right) \right. \\ &\quad \left. + 2 \exp\left(\frac{1}{4\sigma_h^4 (\xi(\tau_i - \hat{\tau}))^2 \bar{\gamma}_b}\right) u\left(-\text{sign}\left(\frac{1}{\xi(\tau_i - \hat{\tau})}\right)\right) \right], \end{aligned} \quad (31)$$

where

$$\alpha_i = \frac{(\xi(\tau_i - \hat{\tau}))^{K-1}}{\prod_{l=1, l \neq i}^K (\xi(\tau_i - \hat{\tau}) - \xi(\tau_l - \hat{\tau}))}, \quad (32)$$

Proof. The worst-case conditional BEP, $\mathbb{P}(e; \hat{\tau}, \mathbf{h})$ for VMISO is given in (26). The process of finding the worst-case conditional BEP, $\mathbb{P}(e; \hat{\tau})$, involves marginalization of $\mathbb{P}(e; \hat{\tau}, \mathbf{h})$ over K PDFs of $\{|h_1|^2, |h_2|^2, \dots, |h_K|^2\}$. However, $\mathbb{P}(e; \hat{\tau})$ can be found easily by marginalizing $\mathbb{P}(e; \hat{\tau}, \mathbf{h})$ over the PDF of random variable, $X = \sum_{k=1}^K |h_k|^2 \xi(\tau_k - \hat{\tau})$. We have shown in Lemma 1 that X has the PDF given in (27). The conditional BEP $\mathbb{P}(e; \hat{\tau}, \mathbf{h})$ is given as

$$\mathbb{P}(e; \hat{\tau}, X) = \frac{1}{2} \text{erfc} \left(\sqrt{\frac{E_b}{N_o}} X \right). \quad (33)$$

$\mathbb{P}(e; \hat{\tau}, X)$ can be marginalized over the PDF of X to get

$$\mathbb{P}(e; \hat{\tau}) = \int_{-\infty}^{\infty} \mathbb{P}(e; \hat{\tau}, X) f_X(x) dx. \quad (34)$$

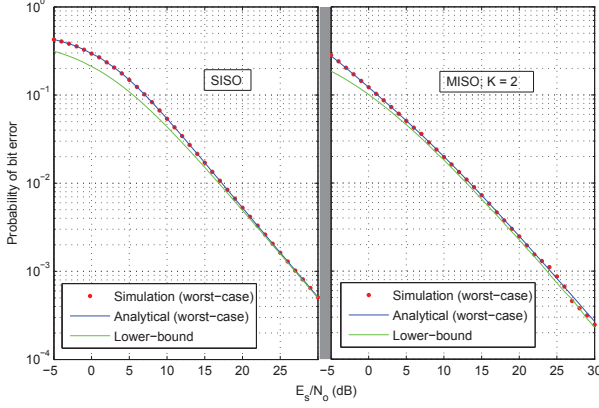


Fig. 2: The average worst-case BEP versus SNR for the SISO and VMISO systems; $K = 2$, $d = 25m$.

The $\mathbb{P}(e; \hat{\tau})$ is found after some mathematical manipulation and is given in (31). ■

The unconditional BEP, $\mathbb{P}(e)$ can be found by marginalizing $\mathbb{P}(e; \hat{\tau})$ over the PDF of $\hat{\tau}$, which is normally distributed with mean $\mu_{\hat{\tau}}$ and $\sigma_{\hat{\tau}}^2$. Therefore, the unconditional BEP, $\mathbb{P}(e)$ is given as

$$\mathbb{P}(e) = \int_{-\infty}^{\infty} \mathbb{P}(e; \hat{\tau}) f_{\hat{\tau}}(\hat{\tau}) d\hat{\tau}, \quad (35)$$

where, $f_{\hat{\tau}}(\hat{\tau})$, is the PDF of $\hat{\tau}$, which is normally distributed with its mean and variance given in Section III and $\mathbb{P}(e; \hat{\tau})$ is given in (31). The integration in (35) is difficult to solve analytically, however, it can be solved by using numerical techniques such as Gauss-Hermite Quadrature integration.

V. RESULTS AND SYSTEM PERFORMANCE

In this section, we present the results corresponding to the SISO and VMISO systems shown in Fig. 1. We use the QPSK modulation employing root-raised cosine pulse shaping filter with roll-off factor, $\beta = 0.25$. We use a training sequence having length, $L_o = 64$. The variance of the channel coefficient is assumed unity i.e., $\sigma_h^2 = 1$. The Monte-Carlo simulation are used for the simulation with 10^5 iterations for each simulation point.

Fig. 2 shows the BEP plot of the SISO system and the MISO system with $K = 2$. It can be seen that the *worst-case* BEP reduces monotonically as the SNR is increased. The simulation result closely matches with the analytical result. A similar trend is observed in the curves labeled as *lower-bound*, which correspond to the BEP for the perfect synchronization case. The *lower-bound* curve for SISO system is found by using (21), while the *lower-bound* curve for MISO is obtained through Monte-Carlo simulation. It is interesting to note that the *worst-case* BEP for the SISO system approaches its *lower-bound* as the SNR increases and this stems from the fact that the variance of the estimator reduces as we increase the SNR. Similarly, the *worst-case* BEP curve for VMISO approaches its *lower-bound* as the SNR is increased but unlike the SISO case, the two curves do not match even at very high SNR

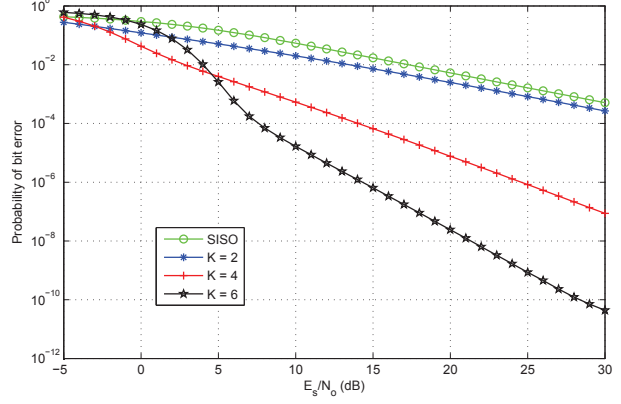


Fig. 3: The average worst-case BEP versus SNR for different number of relays, K ; $d = 25m$.

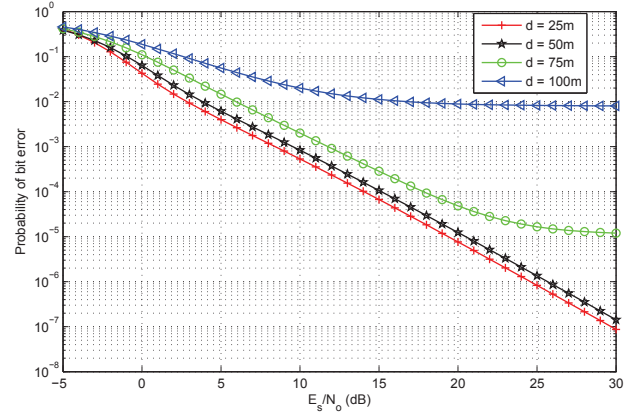


Fig. 4: The average worst-case BEP for different values of distance, d ; $K = 4$.

because of the presence of path delay disparity in VMISO system.

The *worst-case* analytical BEP curves for different number of transmitting relays, K for the VMISO system with $d = 25m$ is shown in Fig. 3. We note that for medium to high SNR, the BEP performance of the VMISO enhances as K increases. The improvement in the performance is due to the increase in array and diversity gains as we increase K . However, at low SNR, the VMISO system with lower number of relays per cluster performs slightly better because the variance of the timing error is directly proportional to K . For comparison purpose, we have shown the *worst-case* analytical curve of the SISO system in this figure. It can be seen that the SISO system performs poorer than the VMISO system at high SNR because it does not incur array or diversity gain. Fig. 3 provides an insight into the required SNR margin to get a specific quality of service (QoS). For instance, if the system is to be operated at $\text{BEP} \leq 10^{-4}$, the VMISO system with four transmitting relays should be operated at 14dB SNR, which is 7dB higher than the SNR required for VMISO system with $K = 6$ for getting the same QoS. Hence, these considerations should be included when designing a VMISO network with imperfect

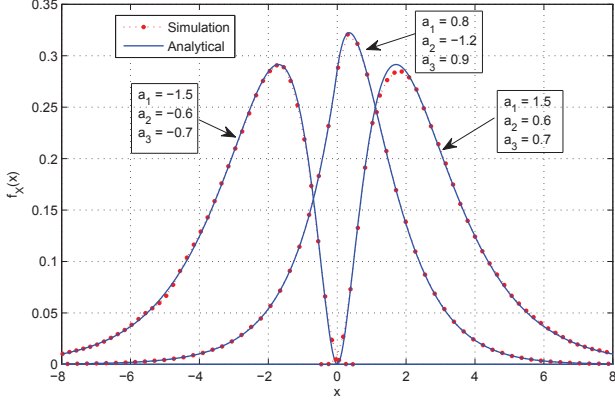


Fig. 5: The PDF of weighted sum of exponential random variables.

synchronization.

The effects of increasing the distance, d on the BEP of VMISO system with $K = 4$ has been shown in Fig. 4. It can be seen that the *worst-case* BEP increases significantly because of the increase in path delay disparity as we increase d . However, at very low SNR, there is no significant change in the BEP because the variance of the timing errors does not change much due to change in d at low SNR as compared to high SNR.

In Fig. 5, the analytical PDF of the weighted sum of exponential random variables provided in Lemma 1 is verified through simulation results. We have shown three different examples, i.e., different coefficients of the exponential random variables, however, we set $\mu = 1$ for all three cases. The simulation results closely match with the analytical curves and it verifies the expression (27) in Lemma 1.

VI. CONCLUSION

The effect of imperfect timing synchronization in a VMISO networks has been investigated. The statistics of the timing errors are modeled and the analytical expressions of the BEP of the network under imperfect synchronization have been derived. The simulation and analytical results were presented. We quantified the results that indicate a degradation in system performance due to imperfect timing synchronization. It has been also observed that by increasing the diversity order or reducing the path delays, the BEP performance can be improved. In future, this analysis should be extended to incorporate the multi-hop propagation in cooperative networks.

APPENDIX A

From (6), we have

$$\mathbb{E}[\hat{\tau}^2] = \mathbb{E}\left[\sum_{k=1}^K \beta_k^2 \hat{\tau}_k^2\right] + \mathbb{E}\left[\sum_{p=1}^K \sum_{\substack{q=1 \\ q \neq p}}^K \beta_p \beta_q \hat{\tau}_p \hat{\tau}_q\right]. \quad (36)$$

Because β_k and $\hat{\tau}_k$ are uncorrelated, the first term in (36) is given as

$$\mathbb{E}\left[\sum_{k=1}^K \beta_k^2 \hat{\tau}_k^2\right] = \sum_{k=1}^K \mathbb{E}[\beta_k^2] \mathbb{E}[\hat{\tau}_k^2]. \quad (37)$$

By using the theorem given in [13] and properties of related distribution, we can have

$$\mathbb{E}\left[\sum_{k=1}^K \beta_k^2 \hat{\tau}_k^2\right] = \frac{2}{K(K+1)} \sum_{k=1}^K (\sigma_k^2 + \tau_k^2). \quad (38)$$

For the second term in (36)

$$\mathbb{E}\left[\sum_{p=1}^K \sum_{\substack{q=1 \\ q \neq p}}^K \beta_p \beta_q \hat{\tau}_p \hat{\tau}_q\right] = \sum_{p=1}^K \sum_{\substack{q=1 \\ q \neq p}}^K \mathbb{E}[\beta_p \beta_q] \mathbb{E}[\hat{\tau}_p \hat{\tau}_q]. \quad (39)$$

According to conclusion given in [13], we have $\mathbb{E}[\beta_p \beta_q] = \frac{1}{K(K+1)}$. Assuming $\hat{\tau}_p$ and $\hat{\tau}_q$ are uncorrelated, (39) is simplified as

$$\mathbb{E}\left[\sum_{p=1}^K \sum_{\substack{q=1 \\ q \neq p}}^K \beta_p \beta_q \hat{\tau}_p \hat{\tau}_q\right] = \frac{1}{K(K+1)} \sum_{p=1}^K \sum_{\substack{q=1 \\ q \neq p}}^K \tau_p \tau_q. \quad (40)$$

By substituting from (38) and (40) into (36), we can get the final expression for $\mathbb{E}[\hat{\tau}^2]$, which is given in (7).

REFERENCES

- [1] J.N. Laneman, D.N.C. Tse, and Gregory W. Wornell, "Cooperative diversity in wireless networks: Efficient protocols and outage behavior," *IEEE Trans. Inf. Theory*, vol. 50, no. 12, pp. 3062–3080, Dec. 2004.
- [2] R. I. Ansari and S. A. Hassan, "Opportunistic large array with limited participation: An energy-efficient cooperative multi-hop network," in *Proc. IEEE ICNC*, Feb. 2014.
- [3] L. Thanayankizil, A. Kailas and M. A. Ingram, "Opportunistic large array concentric routing algorithm (OLACRA) for upstream routing in wireless sensor networks," *ELSEVIER Ad Hoc Networks*, vol. 9, Sept. 2011.
- [4] M. Bacha and S. A. Hassan, "Distributed versus cluster-based cooperative linear networks: A range extension study in Suzuki fading environments," in *Proc. IEEE PIMRC*, Sept. 2013.
- [5] S. A. Hassan and M.A. Ingram, "A quasi-stationary Markov Chain model of a cooperative multi-hop linear network," *IEEE Trans. Wireless Commun.*, vol. 10, no. 7, pp. 2306–2315, July 2011.
- [6] A. Afzal and S. A. Hassan, "Stochastic modeling of cooperative multi-hop strip networks with fixed hop boundaries," *IEEE Trans. Wireless Commun.*, vol. 13, no. 8, pp. 4146–4155, Aug. 2014.
- [7] S. A. Hassan, "Performance analysis of cooperative multi-hop strip networks," *Springer Wireless Personal Communications*, vol. 74, no. 2, pp. 391–400, Jan. 2014.
- [8] X. Li, Y.-C. Wu and E. Serpedin, "Timing synchronization in decode-and-forward cooperative communication systems," *IEEE Trans. Signal Process.*, vol. 57, no. 4, pp. 1444–1455, April 2009.
- [9] A.A. Nasir, H. Mehrpouyan, S.D. Blostein, S. Durrani and R.A. Kennedy, "Timing and carrier synchronization with channel estimation in multi-relay cooperative networks," *IEEE Trans. Signal Process.*, vol. 60, no. 2, pp. 793–811, Feb. 2012.
- [10] M. Hossain, D. Smith, R. Kennedy, and S. Kandeepan, "Effect of timing Error on the performance of BPSK modulation over a fading channel," *IEEE Lett. Commun.*, vol. 14, no. 10, pp. 894–896, Oct. 2010.
- [11] P. Vitthaladevuni and M.-S. Alouini, "Effect of imperfect phase and timing synchronization on the error rate performance of PSK modulations," in *IEEE VTC*, vol. 1, pp. 356–360, 2002.
- [12] S. Jagannathan, H. Aghajan, and A. Goldsmith, "The effect of time synchronization errors on the performance of cooperative MISO systems," in *IEEE GlobeCom Workshops*, pp. 102–107, Nov. 2004.
- [13] R. Heijmans, "When does the expectation of a ratio equal the ratio of expectation," *Statistical Papers*, vol. 40, no. 1, pp. 107–115, Jan. 1999.
- [14] G. L. Stuber, "Principles of Mobile Communication," 3rd Ed. in *Springer*, Sept. 2011.
- [15] M. Trikha, N. Sharma and M. Singhal, "BER performance comparison between QPSK and 4-QA modulation schemes," *MIT International Journal of Electrical and Instrumentation Engineering*, vol. 3, no. 2, pp. 62–66, Aug. 2013.